

Table III. Critical Temperatures and Corresponding Critical Pressures on the Critical Locus of the Binary Systems

system	T/°C	P/MPa
<i>i</i> -C ₄ -H ₂ S	98.0	8.094
	99.0	8.067
	99.0	8.522
	104.4 ^a	6.642 ^a
	110.0	6.088
	125.0	4.785
<i>n</i> -C ₄ -H ₂ S	103.3	7.874
	107.2	7.536
	121.1	6.543
	135.0	5.543
	145.0	4.716

^a Reference 5.

unusual to find a minimum in the critical locus without an azeotrope as in the case of the isobutane-hydrogen sulfide system. This behavior leads to the configuration of the isobars on a temperature-composition diagram as shown on Figure 7. All of the data obtained in this study together with the earlier data of Besserer and Robinson (5) were used in obtaining this cross-plot.

Glossary

K equilibrium ratio, *y/x*
*K*_{H₂S} equilibrium ratio for hydrogen sulfide

*K*_{*n*C₄} equilibrium ratio for *n*-butane
*K*_{*i*C₄} equilibrium ratio for isobutane
P pressure, MPa
T temperature, °C
x mole fraction of component in liquid phase
y mole fraction of component in vapor phase

Registry No. H₂S, 7783-06-4; butane, 106-97-8; isobutane, 75-28-5.

Literature Cited

- Reamer, H. H.; Sage, B. H.; Lacey, W. N. *Ind. Eng. Chem.* **1951**, *43*, 976-981.
- Kay, W. B.; Brice, D. B. *Ind. Eng. Chem.* **1953**, *45*, 615-618.
- Kay, W. B.; Rambosek, G. M. *Ind. Eng. Chem.* **1953**, *45*, 221-226.
- Robinson, D. B.; Hughes, R. E.; Sandercock, J. A. W. *Can. J. Chem. Eng.* **1964**, *42*, 143-146.
- Besserer, G. J.; Robinson, D. B. *J. Chem. Eng. Jpn.* **1975**, *8*, 11-15.
- Reamer, H. H.; Sage, B. H.; Lacey, W. N. *Ind. Eng. Chem.* **1953**, *45*, 1805-1809.
- Reamer, H. H.; Selleck, F. T.; Sage, B. H.; Lacey, W. N. *Ind. Eng. Chem.* **1953**, *45*, 1810-1812.
- Ng, H.-J.; Robinson, D. B. *Fluid Phase Equilib.* **1979**, *2*, 283-292.
- Ng, H.-J.; Kalra, H.; Robinson, D. B.; Kubota, H. *J. Chem. Eng. Data* **1980**, *25*, 51-55.
- Huang, S.-S.; Robinson, D. B. *Fluid Phase Equilib.* **1984**, *17*, 373-382.
- Huang, S.-S.; Robinson, D. B. *J. Chem. Eng. Data* **1985**, *30*, 154-157.
- Robinson, D. B.; Huang, S.-S.; Leu, A.-D.; Ng, H.-J. Research Report RR-57; Gas Processors Association, February 1982.
- Leu, A.-D.; Robinson, D. B. *J. Chem. Eng. Data* **1987**, *32*, 444-447.
- Reid, R. C.; Prausnitz, J. M.; Sherwood, T. K. *The Properties of Gases and Liquids*, 3rd ed.; McGraw-Hill: New York, 1977.

Received for review September 9, 1988. Accepted April 4, 1989.

Vapor-Liquid Equilibrium in the System Carbon Dioxide + *n*-Pentane from 252 to 458 K at Pressures to 10 MPa

Huazhe Cheng,[†] Marla E. Pozo de Fernández,[‡] John A. Zollweg,* and William B. Streett

School of Chemical Engineering, Olin Hall, Cornell University, Ithaca, New York 14853

Equilibrium pressures and compositions for the binary mixture carbon dioxide/*n*-pentane were measured on 10 isotherms from 252 K to the *n*-pentane critical temperature. On each isotherm, the entire pressure range of phase coexistence was covered. The mixture critical line has been located and is shown to be continuous in *P-T-x* space between the critical points of the pure components. Comparisons are made between the experimental results and predictions of the Soave-Redlich-Kwong, Peng-Robinson, Kubic-Martin, and Adachi-Lu-Sugie cubic equations of state. None was able to correlate the data within our estimated experimental error.

Introduction

This study of the binary system carbon dioxide/*n*-pentane is a continuation of experimental investigations of CO₂/*X* systems designed to explore patterns of phase behavior in fluid systems and to obtain accurate data for testing empirical and theoretical methods of data correlation (1, 2). Although there have long been some data for the system of CO₂/*n*-pentane available (3),

a considerable discrepancy was found between the phase compositions measured by Besserer and Robinson (4) and the earlier data of Poettman and Katz (5). Recently two new studies of this system were reported by Leu and Robinson (6) at 135, 160, and 180 °C and by Wu et al. (7) at 38 and 56 °C. The results reported here are distinguished from the other studies by the completeness with which they cover the vapor-liquid equilibrium region of this system.

Experimental Method

Two vapor-recirculating equilibrium apparatuses, designed for use at temperatures from -40 to 70 °C and from 40 to 250 °C and pressures to 200 MPa, have been used. They are described by Pozo and Streett (8) and by Streett and Calado (9), respectively. A schematic diagram of the apparatus for higher temperature measurements is shown in Figure 1. The temperature in the oven is controlled within ±0.02 °C. The apparatus for lower temperature measurements (not shown) is similar. It contained a water/antifreeze bath which was controlled by a Braun Model 1480 BKU proportional temperature controller. Subambient temperatures were obtained by circulating cold water or liquid nitrogen through a heat-exchange coil in the bath. Temperatures in this apparatus could be controlled to within ±0.01 °C. Pressures in both apparatuses were measured with an uncertainty of ±0.007 MPa or ±0.5% (whichever is greater) by using an Autoclave Engineers Model DPS-0021P digital pressure gauge, calibrated in this laboratory against a Ruska dead-weight gauge.

* Author to whom correspondence should be addressed.

[†] Visiting scientist from Beijing Research Institute of Chemical Industry, Beijing, China.

[‡] Present address: Departamento de Termodinámica y Fenómenos de Transferencia, Universidad Simón Bolívar, Caracas 1086-A, Venezuela.

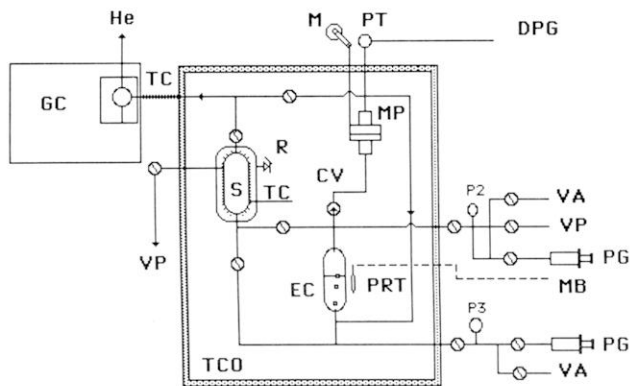


Figure 1. Schematic diagram of vapor-recirculating equilibrium apparatus. Components are labeled as follows: CV, check valve; DPG, digital pressure gauge; EC, equilibrium cell; GC, gas chromatograph; M, motor; MB, Mueller bridge; MP, magnetic pump; P, pressure gauge; PG, pressure generator; PRT, platinum resistance thermometer; PT, pressure transducer; R, relief valve; S, sampling cell; TC, temperature-controlled heater; TCO, temperature-controlled oven; VA, vent to atmosphere; VP, vacuum pump.

The phase compositions were determined by using a Hewlett-Packard Model 5840 gas chromatograph with a thermal conductivity detector. A 20-in. column packed with Porapak Q in 1/8-in.-o.d. stainless steel tubing was used, with helium carrier gas flowing at 25 cm³/min. The column temperature was initially set at 80 °C and programmed to increase at 28 °C/min starting after emergence of the CO₂ peak. The conversion from peak area to composition was determined by using low-pressure samples that were prepared gravimetrically. Because of nonlinearity in the detector response, the final calibration was based on a quadratic relationship between peak area and quantity of each component.

The *n*-pentane was Fisher Infra-red Spectranalyzed grade. The carbon dioxide was supplied by Air Products and Chemicals, Inc., with a stated purity of 99.99%. Neither chemical was further purified.

Results

Vapor and liquid compositions for CO₂/*n*-C₅H₁₂ have been measured on ten isotherms from 252.67 to 458.54 K and at pressures up to the critical region of the mixture. The pressure-temperature extent of the region covered by this study is shown in Figure 2. Results are presented in Table I. Uncertainties in composition are estimated to be 0.002 mole fraction, except in the critical region, where they are probably somewhat larger. The vapor- and liquid-phase envelopes at each of the 10 temperatures are shown as a function of pressure and composition in Figure 3. The equilibrium composition ratios ($K = y/x$) obtained from both phase measurements are also given in Table I and are plotted against $\log P$ in Figure 4.

The critical point on each isotherm above the critical temperature of CO₂ has been obtained by extrapolating the liquid and vapor lines to contact at the top of each loop. A numerical scheme based on the assumption that the tops of the isotherms are approximately cubic in composition was used. The filled squares at the tops of the isotherms in Figure 3 indicate the mixture critical points. The values are presented in Table II.

Comparison with Published Data

Besserer and Robinson (4) reported significant differences between their data and those of Poettman and Katz (5). This study was undertaken to extend the range of measurements because they studied only four isotherms. More recently Leu and Robinson (6) have reported data on additional isotherms. We find that our data are in good agreement with those of

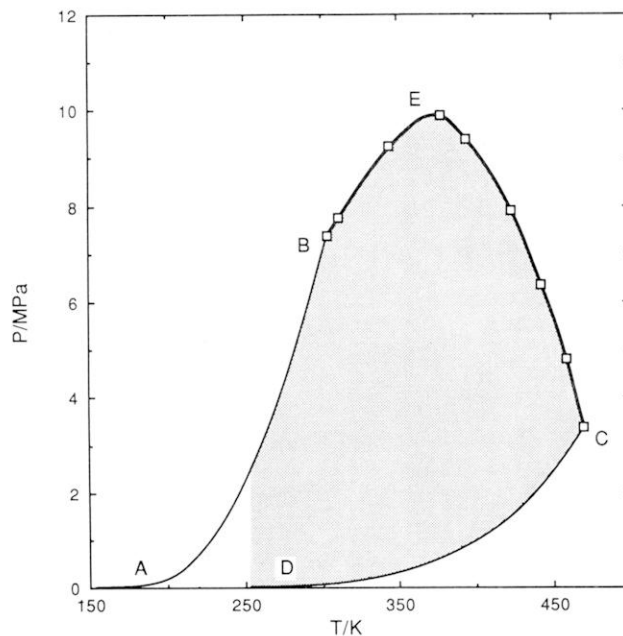


Figure 2. Pressure-temperature diagram for carbon dioxide/*n*-pentane. The shaded area is the P - T region covered in this work. AB and CD are the vapor pressure curves of carbon dioxide and *n*-pentane, respectively, and BEC is the mixture critical line.

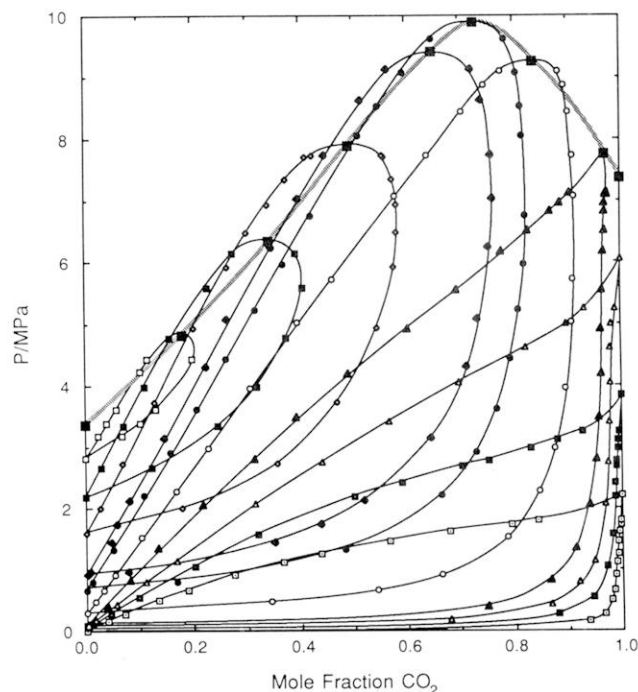


Figure 3. Experimental isotherms for the carbon dioxide/*n*-pentane system. Symbols denote isotherms as follows: □, 252.67 K; ■, 273.41 K; △, 294.09 K; ▲, 311.59 K; ○, 344.34 K; ●, 377.71 K; ◆, 394.31 K; ◇, 423.48 K; ■, 442.53 K; □, 458.54 K.

Besserer and Robinson and Leu and Robinson. Since the experimental temperatures we used were mostly different from those used by Besserer, Leu, and Robinson, we show a direct comparison at only one temperature, 344.34 K, in Figure 5. This figure shows that, within the limits of experimental error, there is good agreement between our data and those obtained by Besserer and Robinson.

Comparison with Equations of State

The vapor and liquid equilibrium compositions at a total of 103 pressures on 10 isotherms were calculated by means of

Table I. Equilibrium Phase Properties of the Carbon Dioxide (1)/*n*-Pentane (2) System

<i>P</i> /MPa	<i>x</i> ₁	<i>y</i> ₁	<i>K</i> ₁	<i>K</i> ₂	<i>P</i> /MPa	<i>x</i> ₁	<i>y</i> ₁	<i>K</i> ₁	<i>K</i> ₂
<i>T</i> = 252.67 K									
0.159	0.0388	0.9375	24.16	0.0650	1.255	0.4368	0.9921	2.271	0.0140
0.276	0.0699	0.9656	13.81	0.0370	1.448	0.5644	0.9928	1.759	0.0165
0.496	0.1342	0.9794	7.298	0.0238	1.600	0.6782	0.9945	1.466	0.0171
0.662	0.1885	0.9849	5.225	0.0186	1.724	0.7925	0.9968	1.258	0.0154
0.910	0.2755	0.9876	3.585	0.0171	1.793	0.8435	0.9968	1.182	0.0204
1.117	0.3654	0.9886	2.705	0.0180					
<i>T</i> = 273.41 K									
0.269	0.0451	0.8798	19.51	0.126	2.668	0.7012	0.9883	1.409	0.0392
0.538	0.0968	0.9443	9.755	0.0617	2.772	0.7517	0.9906	1.318	0.0379
1.048	0.2014	0.9701	4.817	0.0374	2.965	0.8303	0.9920	1.195	0.0471
1.558	0.3206	0.9821	3.063	0.0264	3.103	0.8802	0.9932	1.128	0.0568
2.179	0.5006	0.9868	1.971	0.0264	3.247	0.9274	0.9946	1.072	0.0744
2.406	0.5882	0.9882	1.680	0.0287					
<i>T</i> = 294.09 K									
0.172	0.0165	0.6769	41.02	0.329	3.406	0.5649	0.9776	1.731	0.0515
0.421	0.0542	0.8671	16.00	0.141	4.027	0.6953	0.9797	1.409	0.0666
0.786	0.1111	0.9196	8.277	0.0904	4.592	0.8209	0.9801	1.194	0.111
1.124	0.1671	0.9465	5.664	0.0642	4.999	0.8976	0.9823	1.094	0.173
2.062	0.3153	0.9679	3.070	0.0469	5.240	0.9329	0.9886	1.060	0.170
2.751	0.4409	0.9739	2.209	0.0467					
<i>T</i> = 311.59 K									
0.410	0.0370	0.7458	20.16	0.264	4.930	0.5994	0.9599	1.601	0.100
0.841	0.0790	0.8647	10.95	0.147	5.564	0.6903	0.9642	1.397	0.116
1.365	0.1297	0.9119	7.031	0.101	6.198	0.7746	0.9669	1.248	0.147
2.068	0.2135	0.9372	4.390	0.0798	6.536	0.8258	0.9680	1.172	0.184
2.813	0.3123	0.9495	3.040	0.0734	6.846	0.8664	0.9689	1.118	0.233
3.503	0.3910	0.9557	2.444	0.0727	6.984	0.8853	0.9697	1.095	0.264
4.192	0.4871	0.9602	1.971	0.0776	7.136	0.9026	0.9703	1.075	0.305
<i>T</i> = 344.34 K									
0.469	0.0144	0.3432	23.83	0.666	5.012	0.3960	0.9079	2.293	0.153
0.655	0.0316	0.5409	17.12	0.474	5.723	0.4602	0.9117	1.981	0.164
0.896	0.0534	0.6613	12.38	0.358	7.074	0.5790	0.9135	1.578	0.206
1.530	0.1034	0.7853	7.595	0.240	7.736	0.6382	0.9110	1.427	0.246
2.275	0.1686	0.8452	5.013	0.186	8.439	0.7040	0.9041	1.284	0.324
2.972	0.2266	0.8756	3.864	0.161	8.860	0.7459	0.8959	1.201	0.410
3.944	0.3068	0.8960	2.920	0.150	9.101	0.7768	0.8859	1.140	0.511
<i>T</i> = 377.71 K									
0.786	0.0103	0.1669	16.20	0.842	5.957	0.3693	0.8184	2.216	0.288
1.317	0.0486	0.4825	9.928	0.544	6.750	0.4226	0.8229	1.947	0.307
2.199	0.1076	0.6614	6.147	0.379	8.039	0.5106	0.8167	1.599	0.375
2.896	0.1561	0.7266	4.655	0.324	8.536	0.5482	0.8147	1.486	0.410
3.613	0.2068	0.7658	3.703	0.295	9.073	0.5942	0.8072	1.358	0.475
4.426	0.2625	0.7930	3.021	0.281	9.618	0.6494	0.7855	1.210	0.612
5.212	0.3158	0.8087	2.561	0.280					
<i>T</i> = 394.31 K									
0.986	0.0062	0.0757	12.21	0.930	5.074	0.2616	0.7313	2.795	0.364
1.462		0.3473		0.684	6.267	0.3454	0.7526	2.179	0.378
1.737	0.0561	0.4347	7.749	0.599	7.046	0.3963	0.7582	1.913	0.401
2.130	0.0783	0.5145	6.571	0.527	7.763	0.4441	0.7558	1.702	0.439
3.144	0.1447	0.6426	4.441	0.418	8.632	0.5137	0.7392	1.439	0.536
4.316	0.2224	0.7107	3.196	0.372	9.142	0.5623	0.7190	1.279	0.642
<i>T</i> = 423.48 K									
1.999	0.0253	0.1776	7.020	0.844	6.474	0.3015	0.5818	1.930	0.599
2.510		0.3408		0.709	6.936	0.3393	0.5824	1.716	0.632
2.710	0.0676	0.3571	5.283	0.690	7.343	0.3732	0.5742	1.539	0.679
3.723	0.1287	0.4685	3.640	0.610	7.708	0.4097	0.5566	1.359	0.751
4.916	0.2013	0.5443	2.704	0.571	7.736	0.4239	0.5541	1.307	0.774
5.916	0.2648	0.5768	2.178	0.576					
<i>T</i> = 442.53 K									
2.654	0.0290	0.1230	4.241	0.903	5.578	0.2281	0.4049	1.775	0.771
3.337	0.0710	0.2471	3.480	0.810	6.109	0.2586	0.3998	1.546	0.810
3.971	0.1096	0.3188	2.909	0.765	6.143	0.2756	0.3930	1.426	0.838
4.757	0.1580	0.3739	2.366	0.744					
<i>T</i> = 458.54 K									
3.165	0.0248	0.0682	2.750	0.956	3.833	0.0676	0.1564	2.314	0.905
3.378	0.0402	0.1026	2.552	0.935	4.220	0.1015	0.2117	2.086	0.877
3.599	0.0573	0.1305	2.277	0.922	4.413	0.1153	0.1990	1.726	0.905

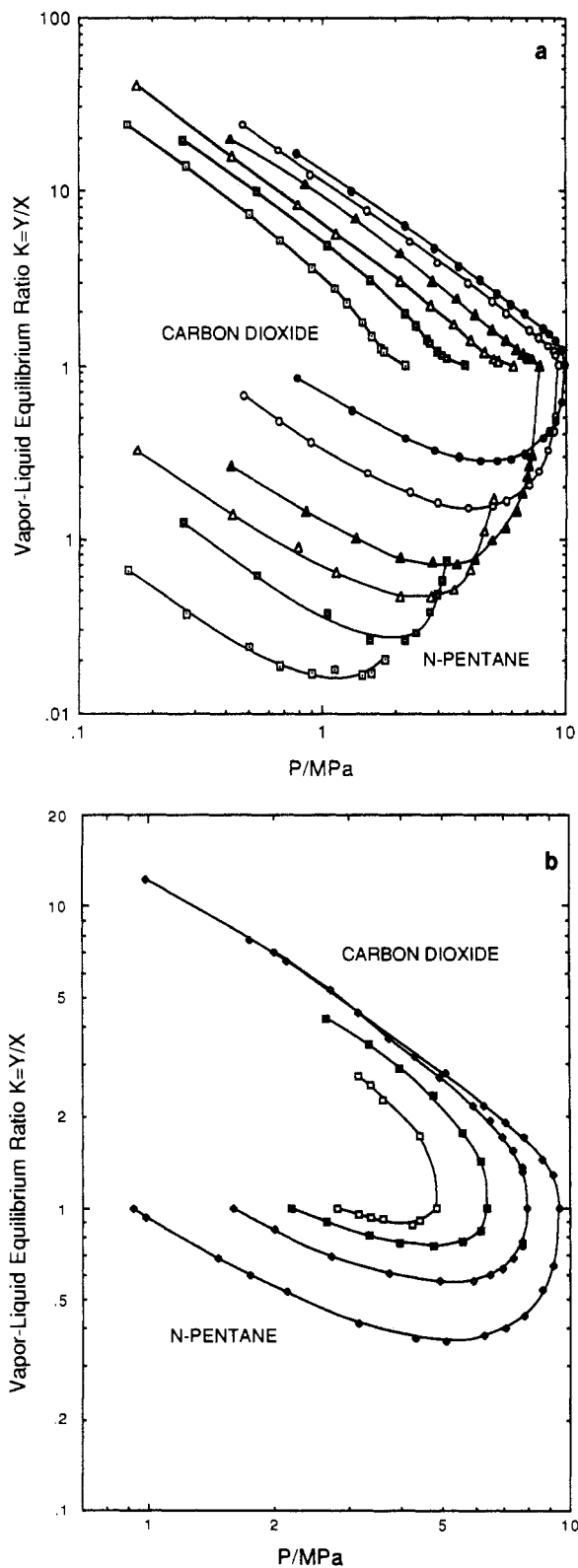


Figure 4. Equilibrium ratios for carbon dioxide/*n*-pentane at temperatures (a) from 252.67 to 377.71 K and (b) from 394.31 to 458.54 K. Symbols are the same as in Figure 3.

Table II. Critical Data for CO₂/*n*-C₅H₁₂ Mixtures

<i>T</i> /°C	<i>P</i> /MPa	<i>x</i> (CO ₂)	<i>T</i> /°C	<i>P</i> /MPa	<i>x</i> (CO ₂)
31.04	7.376	1.000	150.33	7.892	0.492
38.44	7.751	0.972	169.38	6.352	0.344
71.19	9.244	0.837	185.39	4.814	0.181
104.56	9.888	0.727	196.40	3.364	0.000
121.16	9.406	0.648			

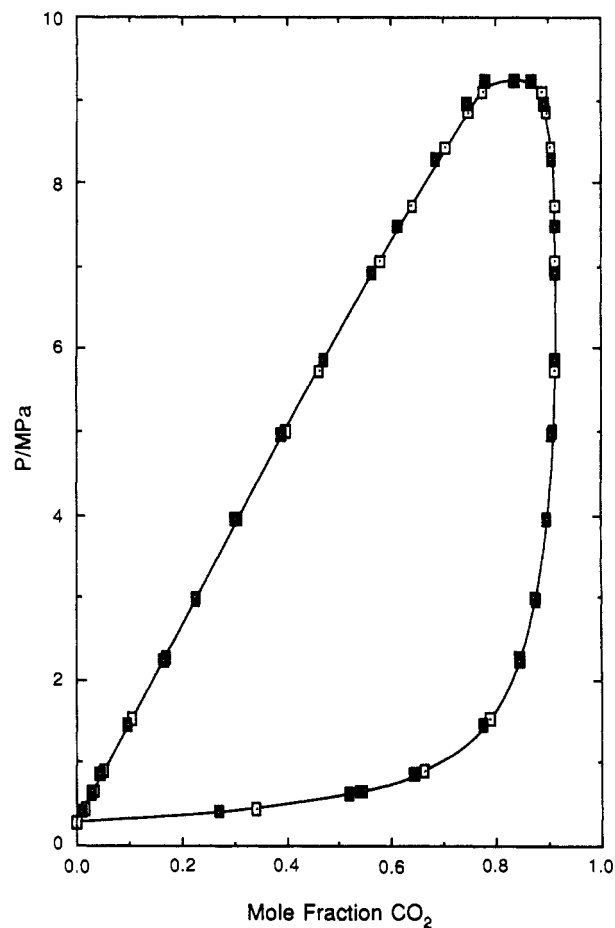


Figure 5. Comparison of experimental data and published data at 344.34 K for carbon dioxide/*n*-pentane: ■, Besserer and Robinson; □, this work.

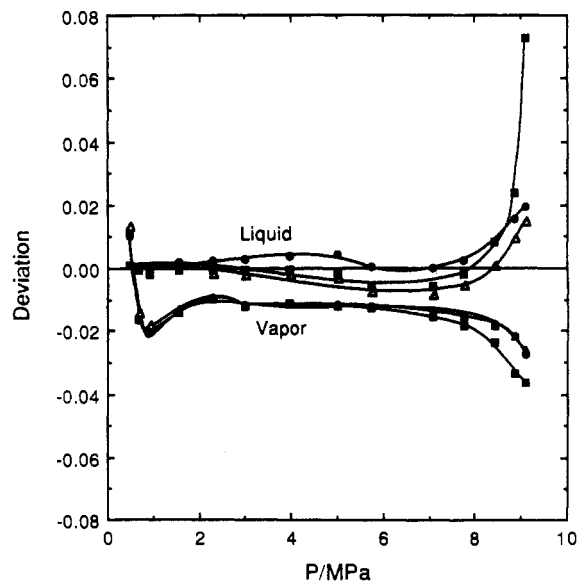


Figure 6. Deviation of predicted phase compositions from experiment. Deviation = $X(\text{calcd}) - X(\text{exptl})$. ●, Peng-Robinson EOS; ■, Kubic-Martin EOS; △, Adachi-Lu-Sugie EOS.

the Soave-Redlich-Kwong (SRK) (10), Kubic-Martin (KM) (11), Adachi-Lu-Sugie (ALS) (12), and Peng-Robinson (PR) (13) equations of state (EOS) and compared with the experimental values. In the calculations, the optimum interaction parameter k_{ij} was determined by minimizing the difference between the calculated and experimental values of liquid composition. This

Table III. Comparison of k_{ij} Used in Different Cubic Equations of State for CO₂/n-Pentane

EOS	k_{ij}	rms(x)	rms(y)	T/K
SRK	0.120	0.0194	0.0022	252.67
PR	0.115	0.0204	0.0021	252.67
ALS	0.115	0.0213	0.0021	252.67
SRK	0.115	0.0129	0.0078	273.41
PR	0.106	0.0124	0.0077	273.41
KM	0.116	0.0269	0.0075	273.41
ALS	0.105	0.0126	0.0077	273.41
SRK	0.106	0.0034	0.0094	294.09
PR	0.100	0.0032	0.0096	294.09
KM	0.124	0.0088	0.0104	294.09
ALS	0.098	0.0035	0.0091	294.09
SRK	0.130	0.0104	0.0084	311.59
PR	0.122	0.0105	0.0096	311.59
KM	0.155	0.0124	0.0123	311.59
ALS	0.121	0.0107	0.0095	311.59
PR	0.121	0.0056	0.0156	344.34
KM	0.159	0.0143	0.0238	344.34
ALS	0.120	0.0061	0.0160	344.34
PR	0.118	0.0031	0.0240	377.71
KM	0.153	0.0050	0.0237	377.71
ALS	0.117	0.0034	0.0247	377.71
PR	0.123	0.0024	0.0265	394.31
KM	0.155	0.0026	0.0244	394.31
ALS	0.122	0.0024	0.0273	394.31
PR	0.138	0.0044	0.0345	423.48
KM	0.167	0.0046	0.0304	423.48
ALS	0.135	0.0041	0.0356	423.48
PR	0.159	0.0049	0.0206	442.53
KM	0.191	0.0049	0.0159	442.53
ALS	0.155	0.0049	0.0220	442.53
PR	0.210	0.0055	0.0375	458.54
KM	0.255	0.0058	0.0357	458.54
ALS	0.190	0.0055	0.0375	458.54

was done because it was observed that the equilibrium liquid compositions were reasonably sensitive to k_{ij} but the vapor compositions were not. Typically, rms(x) would increase by 0.001 when k_{ij} was increased or decreased 0.005 from the optimum value. rms(y) was much less sensitive and typically

was not minimized for the same value of k_{ij} as rms(x). A comparison of interaction parameters and corresponding deviations calculated for four cubic equations of state are presented in Table III. Results for the SRK equation were not included at higher temperatures because they closely paralleled the PR equation. In no case did a cubic equation represent the data within experimental error. A deviation plot of the results at 344.34 K for three of those equations is shown in Figure 6. As can be seen in the figure, the liquid compositions at low and moderate pressures are reasonably correlated, but the predicted vapor compositions are small by about 0.01 mole fraction of CO₂. As is typical with cubic equations of state, the critical region is not accurately represented. The optimum k_{ij} values were reasonably independent of temperature at low temperatures but show a large increase at the highest temperatures. The values of k_{ij} for the Kubic-Martin equation were somewhat larger than for the other three equations, except at the lowest temperature.

Registry No. CO₂, 124-38-9; n-C₅H₁₂, 109-66-0.

Literature Cited

- (1) Tsang, C. Y.; Streett, W. B. *Chem. Eng. Sci.* **1981**, *36*, 993.
- (2) Tsang, C. Y.; Streett, W. B. *J. Chem. Eng. Data* **1981**, *26*, 155.
- (3) Buchner, E. N. *Phys. Chem.* **1906**, *54*, 665.
- (4) Besserer, G. J.; Robinson, D. B. *J. Chem. Eng. Data* **1973**, *18*, 419.
- (5) Postman, F. H.; Katz, D. L. *Ind. Eng. Chem.* **1945**, *37*, 847.
- (6) Leu, A.-D.; Robinson, D. B. *J. Chem. Eng. Data* **1987**, *32*, 444.
- (7) Wu, G.-W.; Zhang, N.-W.; Zheng, X.-Y.; Kubota, H.; Makita, T. *J. Chem. Eng. Jpn.* **1986**, *21*, 25.
- (8) Pozo, M. E.; Streett, W. B. *J. Chem. Eng. Data* **1984**, *29*, 324.
- (9) Streett, W. B.; Calado, J. C. G. *J. Chem. Thermodyn.* **1978**, *10*, 1089.
- (10) Soave, G. *Chem. Eng. Sci.* **1972**, *27*, 1197.
- (11) Kubic, W. L. *Fluid Phase Equilib.* **1982**, *9*, 79.
- (12) Adachi, Y.; Lu, B. C.-Y.; Sugie, H. *Fluid Phase Equilib.* **1983**, *11*, 29.
- (13) Peng, D. Y.; Robinson, D. B. *Ind. Eng. Chem. Fundam.* **1976**, *15*, 59.

Received for review September 19, 1988. Accepted April 17, 1989. We acknowledge support for this research from the National Science Foundation under Grant CPE 8104708. H.C. also acknowledges support from the United Nations Industrial Development Organization (UNIDO).